Optimizing Parameters Contributing to Riveting Quality Using Imperialist Competitive Algorithm and Predicting Objective Function via Three Models MLR, RBF, and ANN-GA

Abbas Fadaei*, Allahyar Gorbanpour
Department of Mechanical Engineering,
University of Bu-Ali Sina, Iran
*Corresponding author E-mail: fadaei@ibasu.ac.ir/ gorbanpour@ibasu.ac.ir

Amir Salarpour
Department of Computer Engineering,
University of Bu-Ali Sina, Iran
E-mail: salarpour@ibasu.ac.ir

Received: 7 September 2015, Revised: 20 December 2015, Accepted: 31 January 2016

Abstract: Metal sheets play an important role in the mechanical design, particularly in the aerospace structures. Various parameters affect the quality of this operation. In this paper, optimization of the parameters contributing to the riveting quality in order to minimize the value of the maximum tangential stress in metal sheets is addressed. hence, the tolerance of the hole diameter in top and bottom sheets, the friction coefficient, and the tolerance of the rivet diameter and the rivet length were considered as the parameters influencing the riveting quality. A total of 64 models were obtained by permutations of the parameters, two at a time. The outputs were determined using finite element method. The objective function for optimization is the maximum tangential stress for which there is no analytical relation. Thus, three methods including the multivariable linear regression (MLR), the artificial neural network model of the radial basis function (RBF) type, and the hybrid model of the artificial neural network and the genetic algorithm (ANN-GA) were employed to model this function. Further, the performance of the three models was compared and the most suitable one was selected to model the objective function. The regression model was used to model the values of the height and the diameter after riveting. The imperialist competitive algorithm is utilized to solve this optimization problem. The obtained value for the maximum tangential stress using the imperialist competitive algorithm is 16368 pounds per square inches. After modification, this value increased to 23440 pounds per square inches using the finite element method. After riveting, the height and diameter of the rivet were respectively measured to be 0.07689 inches and 0.18524 inches.

Keywords: ANN, FEM, GA, Imperialist competitive algorithm, Riveting

Reference: Fadaei, A., Gorbanpour, A., Salarpour, A., 'Optimizing Parameters Contributing to Riveting Quality Using Imperialist Competitive Algorithm and Predicting Objective Function via Three Models MLR, RBF, and ANN-GA', Int J of Advanced Design and Manufacturing Technology, Vol. 9/No. 1, 2016, pp. 1–12.

Biographical notes: A. Fadaei is Assistant Prof. at Mech. Eng. Dep., Bu_Ali Sina Univ., Hamedan, Iran. He received his MSc from Tehran Univ. in 1990, and his PhD in Applied Mech. Design from Bu_Ali Sina Univ. in 2008. **A. Gorbanpour** received his MSc in Mech. Eng. from Bu_ali Sina Univ. in 2013. His research interests include stress analysis, optimization methods and applied design. **A. Salarpour** is currently a PhD student at the Dep. of Computer Eng. in Bu_Ali Sina Univ. in the field artificial intelligence and robotics.

1 INTRODUCTION

Metal sheets play an important role in the mechanical design, particularly in the aerospace structures. The rivet connections are frequently used to connect these sheets. The riveting quality greatly influences the rupture of the rivet and the sheet. A number of factors affect the fatigue of rivet connections. The stress caused during the riveting is one of the factors which markedly influence the fatigue of the rivet connections. Moreover, it is a controllable factor and hence, it is of great interest [1].

In order to measure the tangential and radial stresses in sheets during riveting, the laboratory techniques were employed such as X-ray refraction method [2], the resistive strain gauge technique [3], the ultrasonic technique [4] and the photoelastic method [5]. Since these empirical methods have incurred high costs and had time-consuming, the numerical methods were also used by researchers. The finite element method is a powerful numerical method for simulating the complex deformations of materials. This method has been used for the simulation of the rivet connections since 1990 [3, 5, 6, 7, and 8]. The various parameters affect the value of these stresses and consequently the quality of rivet connections. The individual effect of some of these parameters on the values of the stresses caused during riveting was reported [9]. The genetic algorithm is a technique for solving the optimization problems which is inspired by the nature and its process is carried out based on the biological evolution. The genetic algorithm repeatedly changes a population in the single solutions of the problem. These changes are called evolution. In each step of the evolution, two members of the population were randomly chosen and their children were considered as the next generation. Thus, the population evolves toward an optimal solution. The researchers were used the genetic algorithm method in the recent years in order to optimize the weights of the artificial neural networks [10- 12]. Numerous efforts have been made so far to solve the general optimization problems. The main challenge of the general optimization problem is the fact that the problems which were optimized may have many local optimums. The great numbers of evolutionary algorithms were presented so far to solve the general optimization problem [13, 14]. In the evolutionary algorithms which were presented thus far, the efforts were made to find the optimal response for the optimization problem via modelling the natural evolution process. This is done through the evolution of a population of the potential solutions, similar to the biological population evolution process which can adapt to the environmental changes. The various evolutionary algorithms have been presented for the optimization such as the genetic algorithm [15, 16], the particle swarm optimization algorithm [17-19], and the metal cooling simulation [20- 23]. A new algorithm called the imperialist competitive algorithm [24, 25] has recently been investigated which is not inspired by the natural phenomenon; rather, by the social phenomenon involving humans. The dimensional specifications for the rivet and the sheet as well as the tolerances were selected from the riveting references and the standards in the present research [26, 27]. The axisymmetric finite element method was employed to simulate the riveting in this article. Through different permutations of the input parameters, the 64 models were built for the simulations. The output of the models was determined to be the maximum tangential stress in the sheets. By using regression models as the conventional statistical technique, the various linear and non-linear mathematical relations [28] were tested on the data and the errors were examined. In this research, the linear regression model as well as the non-linear regression model was used to obtain the diameter and the height of the rivet, respectively. The RBF network and the hybrid model of artificial neural network and the genetic algorithm were employed to predict the maximum tangential stress via MATLAB software [29]. An optimization problem was introduced in which the objective function was in form of the hybrid model of the artificial neural network and genetic algorithm. The upper and lower limits of each variable as well as those of the diameter and the height values of the riveted part were considered as the constraints. The imperialist competitive algorithm was employed to solve this optimization problem which had 8 constraints.

2 DESCRIPTION OF PROBLEM

The semi-tubular 100º angled and 2017-T4 aluminium alloy rivet with the nominal diameter of 0.125 inches and the 2024-T3 aluminium alloy sheets with the thickness 0.064 inches were selected for modelling which are frequently used in the aviation industries [26, 27]. The geometrical sizes of the rivet may be observed in Table 1.

Table 1 Geometric parameters used in the rivet modelling [26, 27]

Parameters	Value, inches
Nominal rivet diameter	0.1250
Head rivet diameter	0.2285
Head rivet height	0.0420
Rivet length	0.2500 - 0.3200
Sheet thickness	0.0640
Hole diameter in sheet	0.1285

In this paper, the up and the low tolerance of the hole diameter in the sheets, the friction coefficient, and the tolerance of the rivet diameter and the rivet length were considered as the parameters influencing the riveting quality. The nomenclature of these parameters and their limits are shown in Table 2. A total of 64 models were investigated by the permutations of different models two at a time. The outputs of the finite element model were considered to be the rivet diameter after riveting (D), the rivet height after riveting (H), and the maximum tangential stress, $S_{max,}$ in both sheets which caused the cracks in the sheets [9].

Table 2 Nomenclature of the parameters and their limits [26,27]

Factor	Name	unit	High Limit	Low Limit
X(1)	Tolerance of hole diameter in the top sheet	in	0	+0.008
X(2)	Tolerance of the rivet diameter	in	-0.003	+0.003
X(3)	Rivet length	in	0.025	0.320
X(4)	Riveting force	lbs	1500	3000
X(5)	Tolerance of hole diameter in the bottom sheet	in	0	+0.008
X(6)	Friction coefficient	-	0.2	1.1

3 OBTAINING DATA VIA THE FINITE ELEMENT METHOD

The finite element simulation was performed by the standard ABAQUS software. The boundary conditions for the rivet are demonstrated in Figure 1. Both the sheet and the rivet were defined as deformable bodies in the finite element model. The contact constraint between two contacting surfaces was considered. The element type for meshing the semi-tubular angled rivet was selected CAX4R. The mesh was consisted on the 3965 elements for the rivet, the 3675 elements for the upper sheet and the 3614 elements for the lower sheet after optimizing number of the elements in the meshes. The verification of the model was carried out according to [1]. Each one of the 64 models was examined separately and the aforementioned output was extracted using the finite element method.

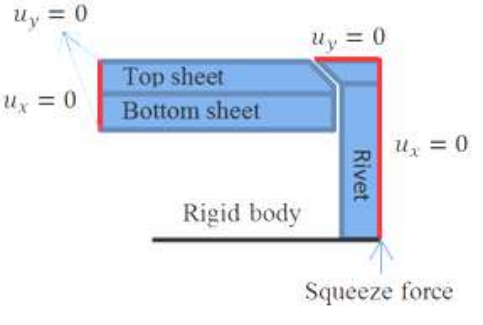

Fig. 1 Boundary conditions

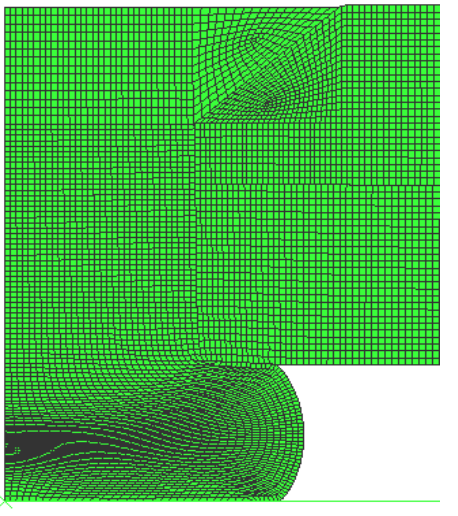

Fig. 2 The deformations for X(1)=X(5)=0, X(2)=0.003, X(3)=0.25, X(4)=1500 and X(6)=0.2

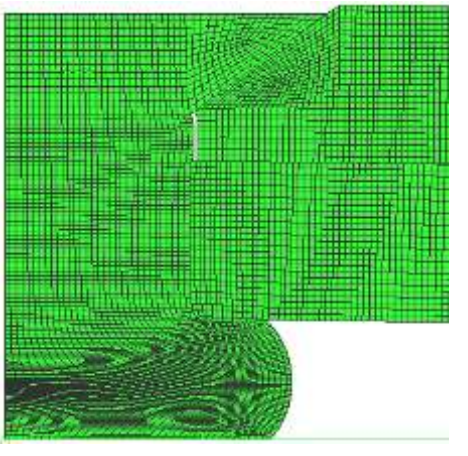

Fig. 3 The deformations for X(1)= 0.008, X(2)=0.003, X(3)=0.25, X(4)=1500, X(5)=0 and X(6)=0.2

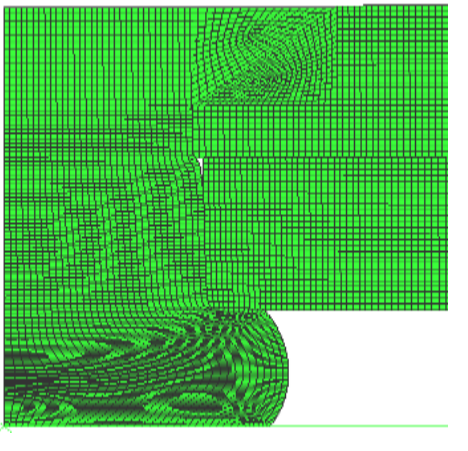

Fig. 4 The deformations for X(1)= 0.008, X(2)=0.003, X(3)=0.25, X(4)=1500, X(5)=0.008 and X(6)=0.2

The material model for the strain hardening was defined as Hollman- Ludwik relation, $\sigma = K\varepsilon^n$ which σ is the actual stress, ε is the actual strain, K is the strength coefficient, 80000 psi for the rivet and 105880 psi for the sheets, and n is the power of the strain hardening, 0.1500 for the rivet and 0.1571 for the sheets. The Young's modulus, the Poisson ratio and the yield stress were selected as 10400 ksi, 0.33 and 24000 psi for the rivet and 10500 ksi, 0.33 and 45000 psi for the sheets, respectively [26, 27]. Figures 2, 3, and 4 show the deformations of three different models from the 64 presented ones.

4 PREDICTING THE MAXIMUM TANGENTIAL STRESS IN THE SHEETS AS THE OBJECTIVE FUNCTION

4.1 USING THE MLR MODEL

Using the regression models is the conventional statistical technique, in this manner, the various linear and the non-linear mathematical relations are tested on the data and the errors are examined. Both the multivariable linear regression (MLR) and the multivariable non-linear regression (MNR) were employed to obtain the s_{max} value. The MLR model was selected which demonstrated the better performance. In addition, the data fit was used to obtain these relations. The coefficient of determination, R^2, and the root mean square error, *RMSE*, were used to assess the regression models which were shown in Eqs. (1) and (2) [10]. In these Eqs., $d_{i(measured)}$ is the measured data, $d_{i(predicted)}$ is the predicted data, $d_{i(mean)}$ is the average value of two data, and n is the number of data:

$$R^2 = 1 - \frac{\sum_{i=1}^{n}(d_{i\,(measured)} - d_{i\,(predicted)})^2}{\sum_{i=1}^{n}(d_{i\,(measured)} - d_{i\,(mean)})^2} \quad (1)$$

$$RMSE = \sqrt{\frac{\sum_{i=1}^{n}(d_{i\,(measured)} - d_{i\,(predicted)})^2}{n}} \quad (2)$$

The coefficient of determination value, R^2, and the root mean square error, *RMSE*, and the mathematical relation obtained from the MLR model for the maximum tangential stress, $S_{max,}$ are shown in Figure 5. The values 0.8189 for R^2 and 3128.4530 for *RMSE* were obtained from Figure 5.

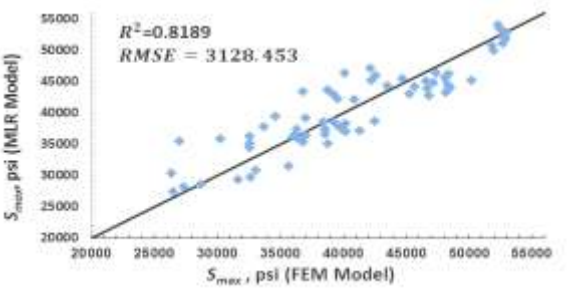

Fig. 5 The finite element and the MLR models results for the he maximum tangential stress

4.2 USING THE ARTIFICIAL NEURAL NETWORK MODEL OF RBF TYPE

The network with the radial basis function (RBF) is illustrated in Figure 6. In this network, the input signals directly were entered into the hidden layer cells. Unlike the MLP networks which have the global activity functions, the local activity functions were used in this network. The number of cells in the hidden layer was obtained by the trial and error. In the output layer, there was only an adder whose the inputs were the outputs of hidden layer cells. The number of output layer cells was selected equal to the number of outputs. In addition, for adjusting the weighted functions upon the training the network, the center of activity functions was also adjusted. The weighted functions were adjusted using the descending gradient method for resulting the least sum of error squared.

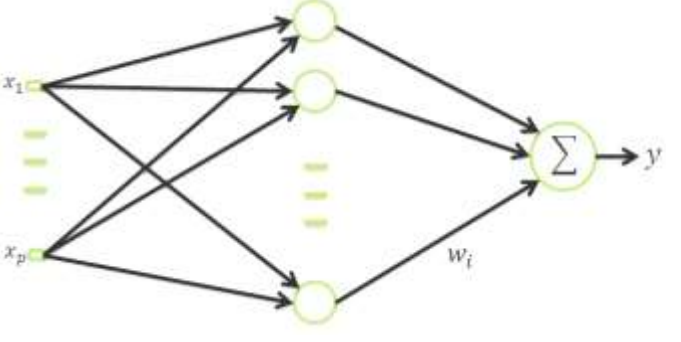

Fig. 6 The network with the radial basis function (RBF)

The function F was chosen by the radial basis functions technique as shown in Eq. (3) [10]:

$$F(x) = \sum_{i=1}^{N} W_i \varphi(\|x - x_i\|) \quad (3)$$

Where, $\varphi_i\ (\|x - x_i\|) : i = 1, 2, ..., N$ are set of N the non-linear functions are called the radial basis function, $\|x - x_i\|$ is defined as the norm of vectors which is normally considered as the Euclidean distance and w_i are the weighted functions. Also, $x_i \in \mathrm{R}^p : i = 1, 2, ..., N$ are the centers of the radial basis functions. In this research, φ, the activity functions for the Gaussian type of the RBF network were selected in form of Eq. (4). As mentioned before, these functions are the local activity functions. In Eq. (4), $\sigma_i : i = 1, 2, ..., N$ are the scale parameter [10]:

$$\varphi_i(\|x - x_i\|) = \exp\left(-\frac{\|x - x_i\|^2}{2\sigma_i^2}\right) \quad (4)$$

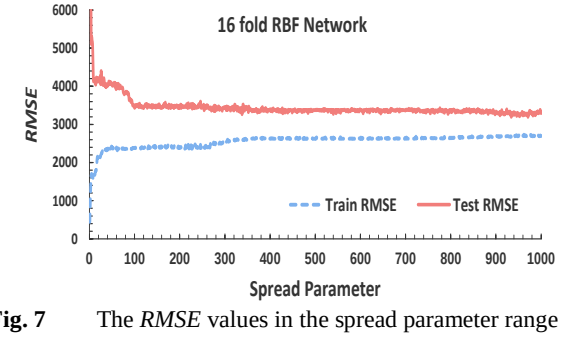

Fig. 7 The *RMSE* values in the spread parameter range for the16 fold RBF network

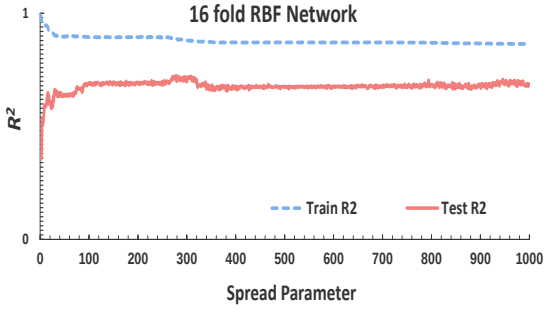

Fig. 8 The R^2 values in the spread parameter range for the 16 fold RBF network

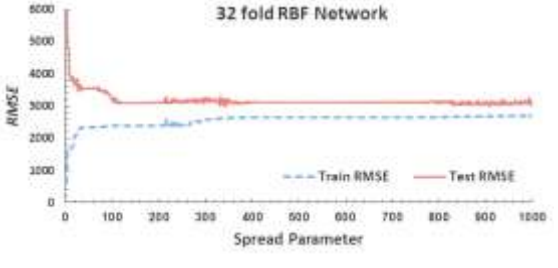

Fig. 9 The *RMSE* values in the spread parameter range for the 32 fold RBF network

using the MATLAB software. For each one of these networks, first the 2 data (16 fold) and second the 4 data (32 fold) were considered as the test data. The test data were tested using the cross validation method; that is, all of the data were tested at least once. The spread parameter was used in the MATLAB software to determine the Gaussian functions. In this research, the value of the spread parameter was considered to vary in the range of 1 to 1000 for all cases [10]. The root mean square error values, *RMSE*, and the coefficient of determination values, R^2, in the spread parameter range for the 16 fold RBF network are shown in Figures 7 and 8, respectively. For the 32 fold RBF network, the root mean square error values, RMSE, and the coefficient of determination values, R2, in the spread parameter range are shown in Figures 9 and 10, respectively. In Figure 10, the test R2 values is either 0 or 1 for the different spread parameters.

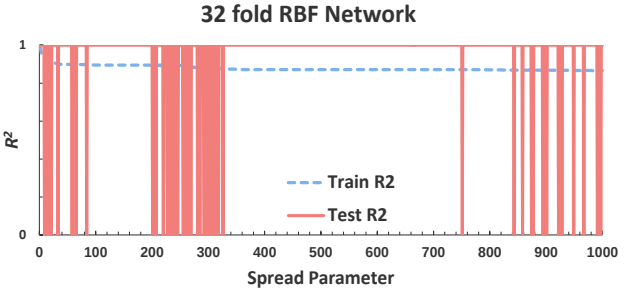

Fig. 10 The R^2 values in the spread parameter range for the 32 fold RBF network

Table 3 The conditions and the results for the 9-selected networks

Network	Spread parameter	Train R^2	Train *RMSE*	Test R^2	Test *RMSE*
16 Fold	1	0.9958	32044.14	0.35513	441.74
16 Fold	278	0.8878	3343.97	0.72584	2489.37
16 Fold	962	0.8650	3279.11	0.70232	2731.61
16 Fold	971	0.8658	3193.49	0.70285	2701.78
16 Fold	994	0.8645	3287.38	0.68725	2710.18
32 Fold	1	0.9927	21720.02	1	619.97
32 Fold	**342**	**0.8740**	**2969.96**	**1**	**2604.99**
32 Fold	986	0.8655	3184.60	1	2714.13
32 Fold	997	0.8653	3083.33	Nan	2697.75

The five networks out of the ones were generated by the 16 fold RBF network and the four networks out of the ones were generated by 32 fold RBF network which were selected, since they presented the better performance according to the *RMSE* and the R^2 criteria. The conditions and the results are demonstrated in Table 3 for these 9 networks. Finally, the 32 fold RBF network with the spread parameter value of 342 was selected which showed the better performance in comparing to others. The comparison between the values of the maximum tangential stress, $S_{max,}$ resulted from the finite element method and obtained from the 32 fold RBF network for the train and the test samples is shown in Figure 11.

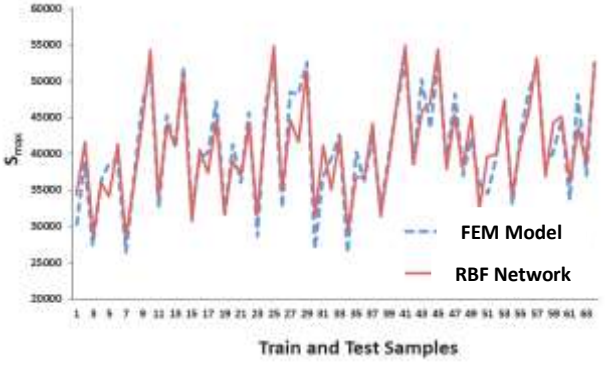

Fig. 11 The comparison between the S_{max} resulted from the finite element method and the 32 fold RBF network

4.3 USING THE HYBRID MODEL OF THE ARTIFICIAL NEURAL NETWORK AND THE GENETIC ALGORITHM (ANN-GA)

In this section, the artificial neural network model is presented to predict the maximum tangential stress in the sheets which lacks the specific analytical relation. The genetic algorithm optimization was employed by the weights and the network bias.

Table 4 The specifications of the hybrid model

Division function	Performance function	Weight/bias learning function	Network training function	Transfer function
'dividerand'	'mse'	'learngdm'	'traingdx'	'tansig'
Combination of mutation	Generation	Train goal	Epochs	-
'standard'	100	0.01	100	-

For this purpose, the four hybrid models of the artificial neural network and the genetic algorithm were designed in the forms of one-layer (1 to 50 neurons), two-layer (1 to 25 neurons), three-layer (1 to 25 neurons), and four layer (1 to 25 neurons). Furthermore, the 44 data for training as well as the 10 data for testing along with the 10 data for the assessment were randomly chosen. The specifications of the hybrid model are shown in Table 4.

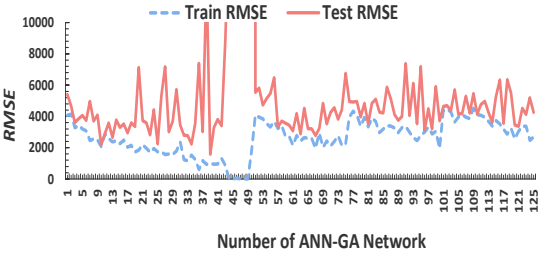

Fig. 12 The train and test values of *RMSE* in 125 structures of the hybrid mode

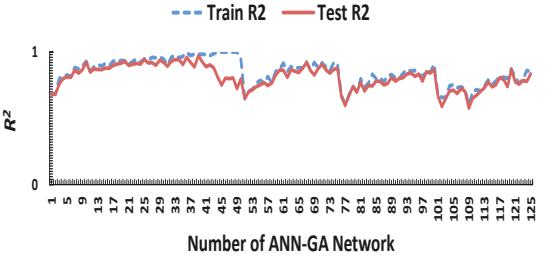

Fig. 13 The train and test values of R^2 in 125 structures of the hybrid mode

Respectively, the train and the test values of *RMSE* and R^2 are demonstrated in Figures 12 and 13 for the 125 structures of the hybrid model. In the Figures, the single-layer ANN-GA for the 1 to 50 networks, the two-layer hybrid model for the 51 to 75 networks, the three-layer hybrid model for the 76 to 100 networks and the four-layer hybrid model for the 101 to 125 networks was employed.

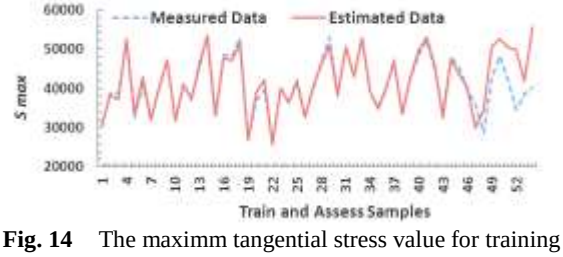

Fig. 14 The maximm tangential stress value for training and assessing the data

The maximum tangential stress value, $S_{max,}$, resulted from the finite element model (the measured data) and obtained from the 39 neurons single-layer hybrid model (the estimated data) for training and assessing the data is shown in Figure 14. In this Figure, the data numbers 1 to 44 for training and numbers 45 to 54 for assessing were used.

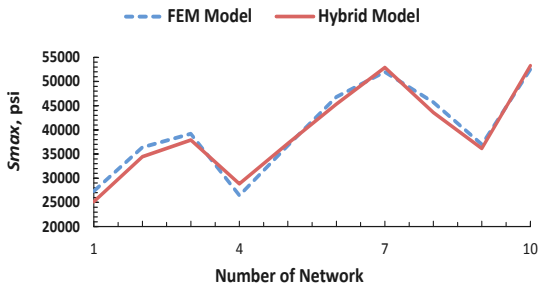

Fig. 15 The maximum tangential stress value for testing the data

In Figure 15, the maximum tangential stress value was determined by the finite element and the 39 neurons single-layer hybrid models for testing data were displayed. Based on the results, the single-layer structure in the hybrid model with the 39 neurons in the hidden layer illustrated the best performance. The value of the determination coefficient, R^2, for the finite element and the hybrid models is shown in Figure 16. This value comprises the acceptable precision.

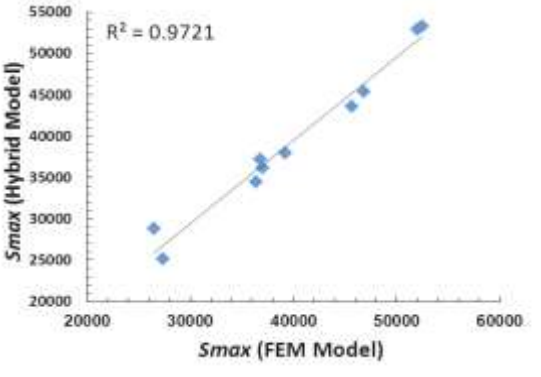

Fig. 16 The value of R^2 in the hybrid model for testing the data

4.4 COMPARISON OF THE THREE METHODS AND SELECTION OF THE MOST SUITABLE ONE

The regression models are the very proper tools in order to obtain the relationship between the input and the output parameters. A linear six-variable relation was used to obtain the value of the maximum tangential stress, S_{max}. The precision of the MLR model precision was not appropriate according to the R^2 and the *RMSE* assessment. The RBF neural network was used as another model to recommend for predicting S_{max}. This model exhibited the better performance compared with the MLR model. One of the famous models in the artificial neural network is the combinational model of the artificial neural network and the genetic algorithm. This hybrid model was employed to predict the maximum tangential stress. The hybrid model demonstrated the better performance compared to the other models.

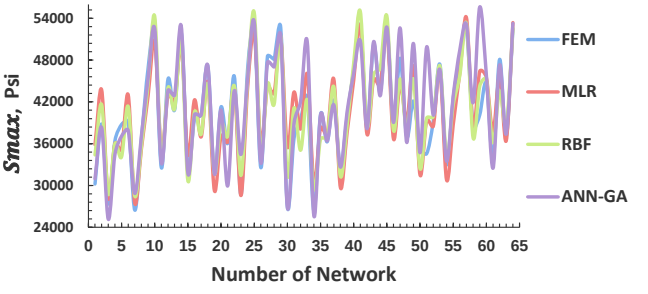

Fig. 17 The values of S_{max} obtained from the finite element method and the three MLR, RBF, and ANN-GA models

Generally, the artificial neural network models showed the better results compared with the regression models for predicting S_{max}. The values of S_{max} obtained from the finite element method and the three MLR, RBF, and ANN-GA models is compared in Figure 17. Moreover, the train and the test data of R^2 and *RMSE* are shown in Table 5 for the three models. As may be seen, the ANN-GA hybrid model presented the better performance in comparison to the other two models. Thus, the ANN-GA hybrid model was selected for modelling the objective function.

Table 5 The values of R^2 and *RMSE* for MLR, RBF and ANN-GA models

Model	Total *RMSE*	Total R^2	Train *RMSE*	Test *RMSE*	Train R^2	Test R^2
ANN-GA	1118.25	0.9789	986.3	1572.3	0.982	0.972
RBF	2567.00	0.8782	2970.0	2605.0	0.874	1.000
MLR	3128.45	0.8189	-	-	-	-

5 OPTIMIZING THE PARAMETERS CONTRIBUTING TO RIVETING QUALITY

5.1 DEFINITION OF THE OPTIMIZATION PROBLEM

The maximum tangential stress, S_{max}, was considered as the objective function which should be minimized. The hybrid model of artificial neural network and the genetic algorithm was used to model this parameter. The up and low limits of the input parameters were considered as the constraints in the optimization problem which are presented in the following format [26, 27]:

$$0 \le X(1) \le 0.008 \quad (5)$$

$$-0.003 \le X(2) \le 0.003 \quad (6)$$

$$0.25 \le X(3) \le 0.32 \quad (7)$$

$$1500 \le X(4) \le 3000 \quad (8)$$

$$0 \le X(5) \le 0.008 \quad (9)$$

$$0.2 \le X(6) \le 1.1 \quad (10)$$

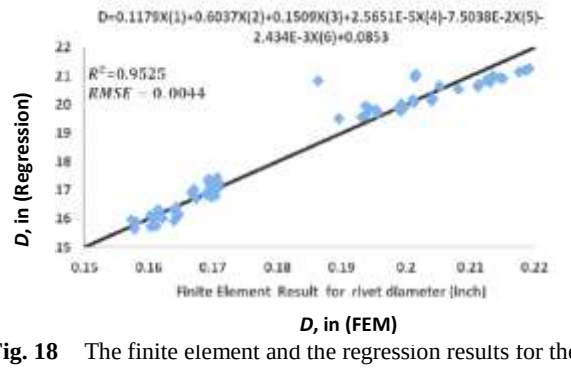

Fig. 18 The finite element and the regression results for the rivet diameter values

The multivariable linear regression and the multivariable non-linear regression were employed to obtain the rivet diameter, *D*, and the rivet height, *H*, after riveting respectively. The finite element and the regression results for the rivet diameter values are shown in the Figure 18. As well as, Figure 19 shows the same results for the height rivet. As shown in these figures, the values of R^2 and *RMSE* indicate the proper precision.

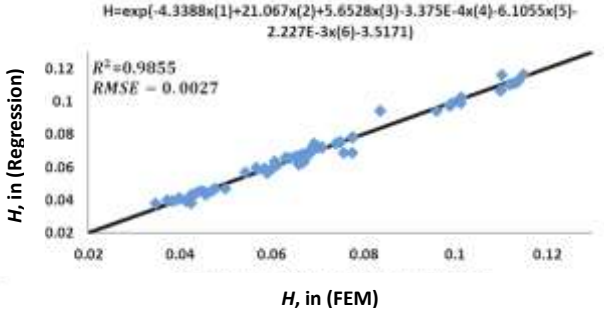

Fig. 19 The finite element and the regression results for the rivet height values

The up and low limits for the rivet diameter after riveting, *D*, was selected as the constraint in the optimization problem [1]. Using the regression method, this value was determined as Eq. (11):

$$0.1719 \le 0.1179X(1) + 0.6037X(2) + 0.1509X(3) + 2.5651E-5X(4) - 7.5038E-2X(5) - 2.4340\,\mathrm{E}-3X(6) + 0.0853 \le 0.2188 \quad (11)$$

The value of the height rivet after riveting, *H*, was chosen as another constraint in the optimization problem. It should be in the range of the up and low limits [1].This value was obtained from the regression method as Eq. (12):

$$0.0469 \le Exp[-4.3388X(1) + 21.0670X(2) + 5.6528X(3) - 3.3750E-4X(4) - 6.1055X(5) - 2.2270E-3X(6) - 3.5171] \le 0.0781 \quad (12)$$

5.2 IMPERIALIST COMPETITIVE ALGORITHM FOR THE OPTIMIZATION PROBLEM

5.2.1 AN INTRODUCTION TO THE IMPERIALIST COMPETITIVE ALGORITHM

There are number of individuals in the genetics algorithm which constitute a population. Under the effect of the combination and the mutation operators, the population individuals move within the search space to select the best answer. The goal in optimization is to find an optimal answer in terms of the problem variables. An array of problem variables which should be optimized is created. This array is called a chromosome in the genetic algorithm. Here, it is called the country. In an N_{var}–dimensional optimization problem, a country is a $1\times N_{var}$ array. This array is defined as Eq. (13) [24]:

$$Country = \{p_1, p_2, p_3, ..., p_{N_{var}}\} \quad (13)$$

All of the countries are categorized into two groups which are called the colonizer and the colony. Every empire is comprised of a colonizer and the countries under its colony. The cost of a country may be calculated using Eq. (14) [24]:

$$cost_i = f(country_i) = f(p_1, p_2, p_3, ..., p_{N_{var}}) \quad (14)$$

Moreover, the total cost of an empire which is equal to the cost of the colonizer plus a percentage, ξ, of the colonies mean cost, may be calculated using Eq. (15) as the following [24]:

$$T.C._n = Cost(imperialist_n) + \xi.Mean\{Cost(colonies_n)\} \quad (15)$$

A total of the $N_{country}$ countries are created in order to initiate the algorithm. A total of N_{lmp} out of the best countries are selected as the imperialist countries. The remaining the N_{col} countries constitute the colonies. The colonies of each imperialist country are determined in accordance with its power. To do so, their normalized cost is initially assumed to estimate by Eq. (16) [24]:

$$C_n = \underset{i}{Max}\{c_i\} - c_n \quad (16)$$

The normalized power of an imperialist country is the ratio of colonies run by that imperialist country. After calculating the normalized cost, the relative normalized power of each imperialist country is calculated according to Eq. (17) [24]:

$$p_n = \left| \frac{c_n}{\sum_{i=1}^{N_{imp}} c_i} \right| \tag{17}$$

Therefore, the initial number of the colonies of an imperialist is determined by Eq. (18) [24]:

$$N.C._n = Round\{ p_n.(N_{col}) \} \tag{18}$$

The establishment of first empires is demonstrated in the Figure 20. As shown in this Figure, the larger empires include more colonies. The number 1 imperialist country has the strongest empire and the greatest number of the colonies.

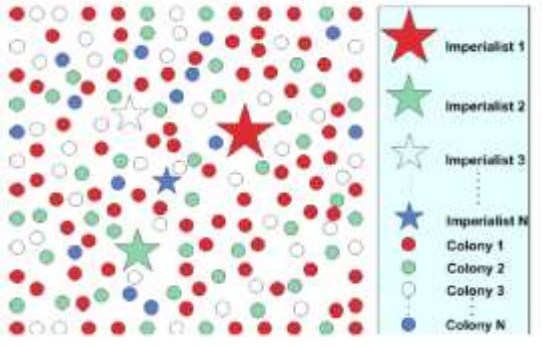

Fig. 20 The establishment of first empires [24]

By adopting a policy of the absorption (assimilation) in line with the different axes of optimization, the colonizers attract the colonies toward themselves. This part of the colonization process in the optimization algorithm is modelled in form of the movement of colonies toward the imperialist country. An overview of this movement is represented in Figure 21. As shown, the imperialist country attracts the colony along the cultural and the lingual axes.

In Figure 21, if the distance between the colony and the colonizer is *d*, the movement of the colony will be as much as *x* toward the location of the corresponding colonizer. This movement is of course deviated at an angle of θ, where the values of *x* and θ are chosen randomly. The value changes of the angle θ and the movement *x* occurs in the ranges $[\gamma, -\gamma]$ and $[0, \beta d]$, respectively. The values γ and β as algorithm parameters are recommended to be 45 degrees and 2, respectively [25].

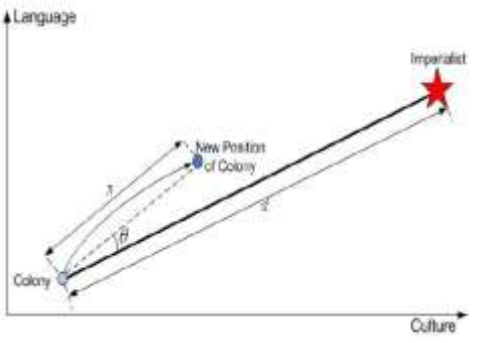

Fig. 21 The movement of colonies toward their relevant imperialist [24]

Any empire which is unable to gain the power and loses the competitiveness will be eliminated from the course of the imperialistic competitions. In the course of time, the weak empires lose their colonies and the stronger empires seize them and increase their power. The stronger empire is more likely to seize the colonies. At first, the total normalized cost of the empire is calculated using its total cost by Eq. (19) [24]:

$$N.T.C._n = \underset{i}{Max}\{T.C._i\} - T.C._n \tag{19}$$

After determining the total normalized cost, the probability of a colony is calculated for which the empires are competing using Eq. (20) [24]:

$$p_{p_n} = \left| \frac{N.T.C._n}{\sum_{i=1}^{N_{imp}} N.T.C._i} \right| \tag{20}$$

The colony is given to one of the empires using a mechanism such as the roulette wheel. An overview of this algorithm is shown in Figure 22. In accordance with this algorithm, the larger empires are more likely to get hold of the colonies of other empires.

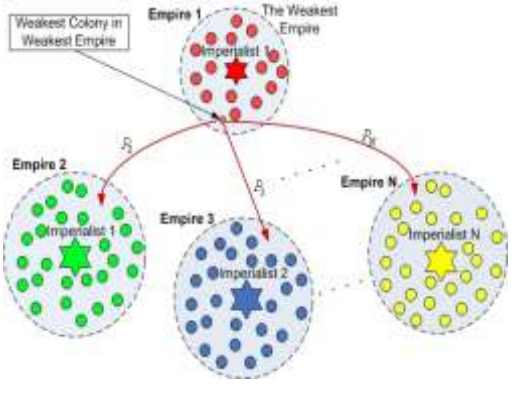

Fig. 22 Imperialistic competition [24]

5.2.2 THE SOLUTION OF THE OPTIMIZATION PROBLEM

The imperialist competitive algorithm [24, 25] is used to solve the optimization problem. The number of countries, empires, and decades are considered to be 100, 10, and 100, respectively. The value of maximum tangential stress obtained from the imperialist competitive algorithm was estimated 16386 psi. After modification using the finite element method, this value increased to 23440 psi. This difference is due to the error in predictions by the artificial neural network and the regression. The maximum tangential stress after modification using the finite element method is shown in Figure 23. The average and the minimum cost for all the empires in 100 iterations of the algorithm is demonstrated in Figure 24. The optimal values for the design variables obtained from the imperialist competitive algorithm are shown in Table 6.

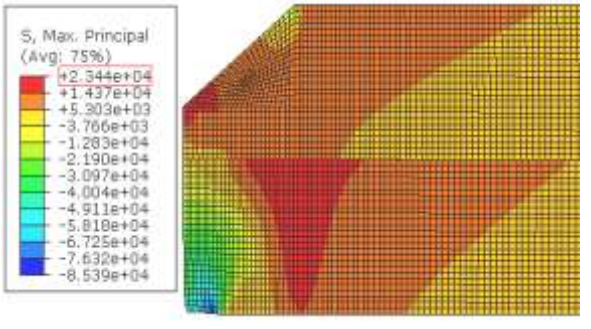

Fig. 23 The maximum tangential stress

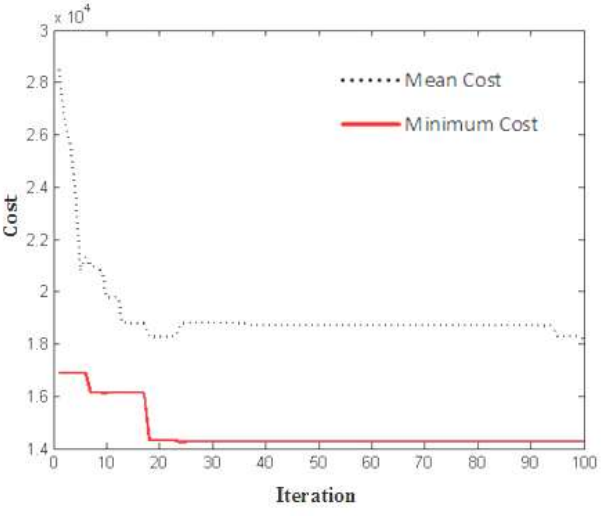

Fig. 24 The mean and minimum cost for all empires in 100 iterations of the algorithm

Table 6 The optimal values for the design variables

Design Variables	X(1)	X(2)	X(3)	X(4)	X(5)	X(6)
Optimal Values	0.000	0.003	0.280	2000	0.000	0.400

The optimal value for the rivet diameter, *D*, was obtained 0.18524 inches. The deformation contour in direction of the rivet radius is indicated in Figure 25. Using the maximum value U_1 and Eq. (21) [26, 27], the rivet diameter value after riveting may be calculated:

$$D = D_0 + X(2) + 2U_{1\,max} = 0.125 + 0.003 + 2 \times 0.0286 = 0.1852 \quad (21)$$

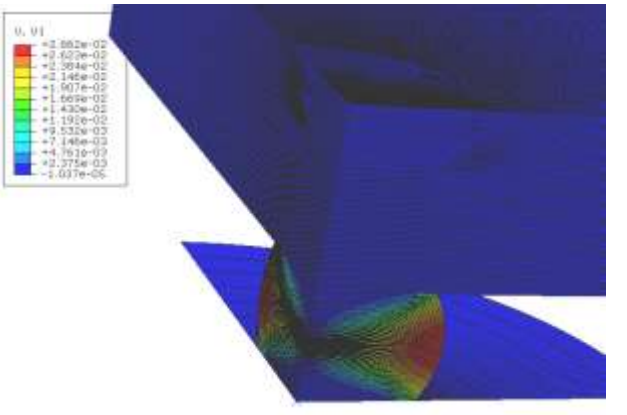

Fig. 25 The deformation contour in direction of the rivet radius

The optimal value for the rivet height, *H*, was obtained 0.07689 inches. The deformation contour in direction of the rivet length is displayed in Figure 26. Using the maximum value U_2 and Eq. (22) [26, 27], the rivet height value after riveting may be determined:

$$H = X(3) - 2t - U_{2\,max} = 0.280 - 2 \times 0.064 + 0.0751 = 0.0769 \quad (22)$$

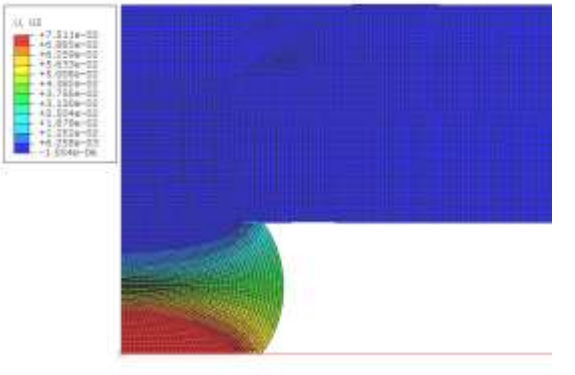

Fig. 26 The deformation contour in direction of the rivet length

6 CONCLUSION

The tangential stresses arising in sheets during riveting are important factors leading to cracks in sheets. Various parameters contribute to the amount of these stresses. The riveting force, the tolerance of hole diameter in the top sheet, the tolerance of hole diameter in the down sheet, the friction coefficient, the tolerance of the rivet diameter and the rivet length were studied as the influential parameters.

The up and low limits for each parameter were considered and the 64 (2^6) models were built via the permutations of the different models two at a time. The maximum tangential stresses in sheets, the diameter and the length of the rivet after riveting were considered as the output of the models. They were obtained using the axisymmetric finite element method. The three MLR, RBF, and ANN-GA methods were used to predict the maximum tangential stress as the objective function in the optimization problem.

With respect to the regression model, the several linear and the non-linear mathematical relations were investigated to model the maximum tangential stress from among which a six-variable linear mathematical relation, which showed less error, was selected. Although the relations were simple but they had the high *RMSE* value; therefore could not be used in modelling the objective function. Another model examined for predicting the objective function was the RBF neural network. A total of the 2000 RBF models with the spread values varying between 1 and 1000 were designed in order to arrive at the appropriate RBF model. In these models, the 2 or 4 test data were switched in turn using the cross validation method. The RBF model with the two test data which performed better was selected from among these models. The spread value was considered to be 342 for the RBF model. The *RMSE* value of this model decreased compared to that of the MLR model; however, the *RMSE* value in the RBF model was still not suitable for the objective function.

Finally, the total of 125 hybrid models of the artificial neural network and the genetic algorithm were used in order to predict the maximum tangential stress. After analysing the performance of these models via the two R^2 and *RMSE* criteria, the single-layer hybrid model with 39 neurons was selected to predict the objective function. The regression method was employed to model the rivet diameter, *D*, and the rivet height, *H*, after riveting.

The two six-variable linear and non-linear relations were obtained for modelling these two values. The up and low limits for *D*, *H*, and the six variables of the problem were considered as the constraints of the optimization problem. In the end, the optimization problem was solved with the objective function in form of the hybrid model of the artificial neural network and the genetic algorithm, two non-linear constraints and six other constraints (the boundary conditions of the problem variables).

The imperialist competitive algorithm (ICA) was employed to this problem and the optimal values were obtained for the problem variables. The obtained value for the maximum tangential stress using the imperialist competitive algorithm was determined 16368 psi. After the modification, this value increased to 23440 psi using the finite element method. This error value was evaluated as the error in the prediction by the artificial neural network and the regression. The least value eligible in the numerical data is 26958 psi. The values of 0.07689 inches and 0.18524 inches were obtained for *H* and *D* respectively. Also, these values were in the desired range. In addition, the power of the imperialist competitive algorithm in solving the optimization problems is demonstrated, in which there is not any analytical relation for the objective function and the constraints.

REFERENCES

[1] Cheraghi, S.H., "Effect of Variations in the Riveting Process on the Quality of Riveted Joints," Journal of Advanced Manufacturing Technology, Vol. 39, No. 11-12, 2008, pp. 1144-1155.

[2] Fitzgerald, T. J., and Cohen J. B., "Residual Stresses in and around Rivets in Cl Aluminum Alloy Plates," Materials Science and Engineering, A188, 1994, pp. 51-58.

[3] Langrand, B., Deleotombe, E., Markiewicz, E. and Drazetic P., "Riveted Joint Modeling for Analysis of Airframe Crashworthiness," Finite Elements in Analysis and Design, Vol. 48, 2001, pp. 21-44.

[4] Ryzhova, T. B., "Estimation of the Reliability of Ultrasonic Quality Control of Riveted Joints with Clearance," Russian Journal of Nondestructive Testing, Vol. 30, 1994, pp. 418-421.

[5] Muller, R.P., "An Experimental and Analytical Investigation on the Fatigue Behavior of Fuselage Riveted Lap Joints," Ph.D. Thesis, Delft University of Technology, Delft, Netherlands, 1995.

[6] Szolwinski, M. P. and Farris, T. N., "Linking Riveting Process Parameters to the Fatigue Performance of Riveted Aircraft Structures," Journal of Aircraft, Vol. 37, No.1, 2000, pp. 130-137.

[7] Deng, X. and Hutchinson, J. W., "The Clamping Stress in a Cold Driven Rivet," Journal of Mechanical Sciences, Vol. 40, 1998, pp. 683-694.

[8] Blanchot, V. and Daidie, A., "Study and Numerical Characterization of a Riveting Process," Journal Material Forming, Vol. 1, No. 1, 2008, pp. 1275 –1278.

[9] Amarendra, A. and Johnson, W. S., "Effect of Interference on the Mechanics of Load Transfer in Aircraft Fuselage Lap Joints," Journal of Engineering Materials and Technology, Vol. 129, 2007, pp. 356-366.

[10] Basheer, I. A. and Hajmeer, M., "Artificial Neural Networks: Fundamentals, Computing, Design, and Application," Journal of Microbiological Methods, Vol. 43, 2000, pp. 3-31.

[11] Goldberg, D. E. and Forrest, S., "Genetic Algorithms in Search, Optimization, and Machine Learning," Addison-Wesley, Reading, MA, 1989.

[12] Fiszelew, A., Britos, P., Ochoa, A., Merlino, H., Fernandez, E. and Garcia-Martinez, R., "Finding Optimal Neural Network

Architecture using Genetic Algorithms," Advances in Computer Science and Engineering Research in Computing Science, Vol. 27, 2007, pp.15-24.

[13] Sarimveis, H. and Nikolakopoulos, A., "A Line up Evolutionary Algorithm for Solving Nonlinear Constrained Optimization Problems," Computers and Operations Research, Vol. 32, No. 6, 2005, pp. 1499– 1514.

[14] Abbass, H. A., Sarker, R. and Newton C., "PDE: A Pareto-Frontier Differential Evolution Approach for Multi-Objective Optimization Problems," Proceedings of the Congress on Evolutionary Computation, Vol. 2, 2001.

[15] M¨uhlenbein, H., Schomisch, M. and Born, J., "The Parallel Genetic Algorithm as Function Optimizer," Proceedings of The Fourth International Conference on Genetic Algorithms, University of California, San Diego, 1991, pp. 270-278.

[16] Melanie, M., An Introduction to Genetic Algorithms, A Bradford Book, The MIT Press, Cambridge, Massachusetts, London, England, 1999.

[17] Angeline P.J., "Evolving fractal movies," Proceedings 1st Annual Conference on Genetic Programming, MIT Press, Cambridge, MA, pp. 503– 511, Springer Verilog, Heidelberg, 1997.

[18] Kennedy, J. and Eberhart, R. C., "Particle Swarm Optimization," Proceedings of IEEE International Conference on Neural Networks, Piscataway, IEEE, 1995, pp. 1942–1948.

[19] Yang, X., Yuan, J., Yuan, J. and Mao, H., "A Modified Particle Swarm Optimizer with Dynamic Adaptation," Applied Mathematics and Computation, Vol. 189, No. 2, 2007, pp. 1205-1213.

[20] Tokuda, I., Aihara, K. and Nagashima, T., "Adaptive annealing for chaotic optimization," Physical Review Letters, Vol. 81, No. 10, 1998, pp. 2156–2159.

[21] Ingber, L.A., "Simulated Annealing: Practice versus Theory," Mathematical and Computer Modelling, Vol. 18, No. 11, 1993, pp. 29–57.

[22] Cardoso, M.F., Salcedo, R. L., Azevedo, S. F. and Barbosa, D., "A Simulated Annealing Approach to the Solution of MINLP problems," Computers and Chemical Engineering, Vol. 21, No. 12, 1997, pp. 1349–1364.

[23] Kirkpatrick, S., Gelatt, C. D. and Vecchi, M. P., "Optimization by Simulated Annealing," Science, Vol. 220, 1983, pp. 671-680.

[24] Esmaeil, A.G. and Lucas, C., "Imperialist Competitive Algorithm: An Algorithm for Optimization Inspired by Imperialistic Competition," Proceedings of the IEEE Congress on Evolutionary Computation, 2007, pp. 4661–4667.

[25] Esmaeil, A. G., Hashemzadeh, F. and Rajabioun R., "Colonial Competition Algorithm: A Novel Approach for PID Controller Design in MIMO Distillation Column Process," Journal of Computer Applications, Vol. 1, No. 3, 2008, pp. 337–355.

[26] Military Standardization Handbook, Metallic materials and elements for aerospace vehicles structures, Defense Automated Printing Services, Philadelphia, (MIL-HDBK-5G), 1994.

[27] Reithmaier, L., Standard aircraft handbook, Tab Aero 5th ed., Blue Ridge Summit, PA, 1991.

[28] Paliwal, M. and Kumar, U. A., "Neural Networks and Statistical Techniques: A Review of Applications," Expert Systems with Applications, Vol. 36, No. 1, 2009, pp. 2-17.

[29] Demuth, H., Beale, M., Neural Network Toolbox User's Guide for Use with MATLAB, Math Works Inc., 2002.